analytical chemistry

pubs.acs.org/ac Article

Arrest of CRISPR-Cas12a by Nonspecific Single-Stranded DNA for Biosensing

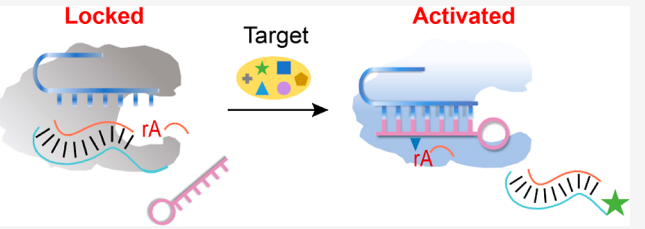
Yue Liu,[⊥] Yunping Wu,[⊥] Yi Liu,[⊥] Qiang Zhang, Hong Yuan, Shen Li, Zhi Li, Bo Wang, Yangyang Chang,* and Meng Liu*

Cite This: https://doi.org/10.1021/acs.analchem.4c07081 Read Online

ACCESS | Metrics & More | Article Recommendations | Supporting Information

Downloaded via SHANGHAI NORMAL UNIV on April 23, 2025 at 13:36:38 (UTC).
See https://pubs.acs.org/sharingguidelines for options on how to legitimately share published articles.

ABSTRACT: CRISPR-Cas technologies have emerged as powerful biosensing tools for the sensitive and specific detection of non-nucleic acid targets. However, existing biosensing strategies suffer from poor compatibility across diverse targets due to the complicated engineering of crRNA and DNA activator required for the CRISPR-Cas activity regulation. Herein, we report a novel and straightforward strategy for designing CRISPR-Cas12a-based biosensors that function by switching structures from single-stranded (ss)DNA/CRISPR-Cas12a assembly to DNA activator/CRISPR-Cas12a complex in the presence of target bacterium. The strategy begins with a ssDNA assembly made of a trans-acting RNA-cleaving DNAzyme (tRCD) and an RNA/DNA chimeric substrate (RCS). The ssDNA assembly has the ability to bind Cas12a nonspecifically, thus indeed blocking the CRISPR-Cas12a activity. By exploiting the specific recognition and cleavage capacities of tRCD for RCS in the presence of a target, the target-bound tRCD and the cleaved RCS are released from Cas12a, thus restoring the CRISPR-Cas12a activity. This method has been successfully applied for the sensitive (detection limit: 10^2 CFU/mL) detection of *Escherichia coli* (*E. coli*, EC) and *Burkholderia gladioli* (*B. gladioli*, BG). For the blind testing of 30 clinical urine samples, it exhibited 100% sensitivity and 100% specificity in identifying *E. coli*-associated urinary tract infections (UTIs).



INTRODUCTION

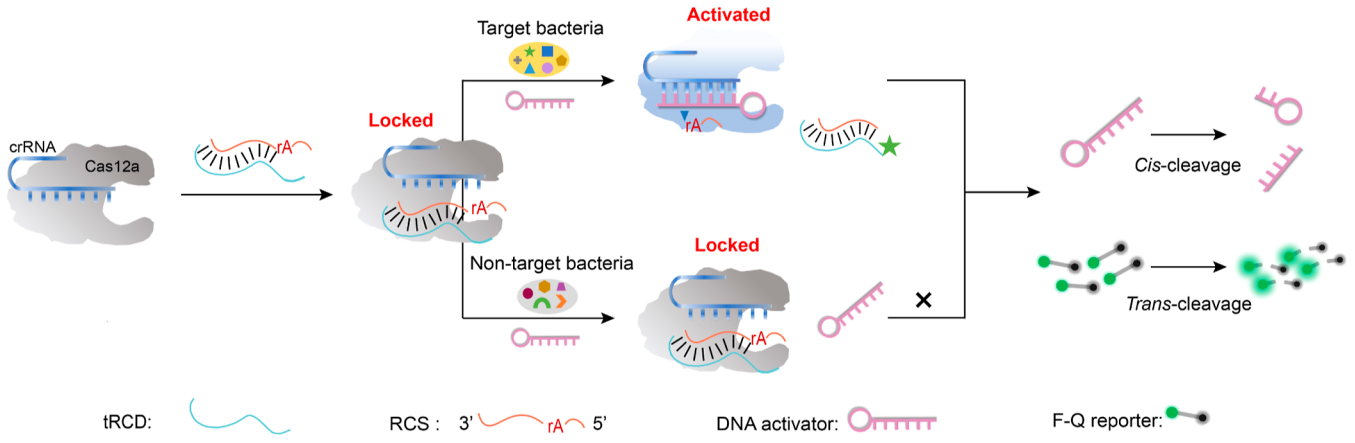
The clustered regularly interspaced short palindromic repeats (CRISPR RNA, crRNA) and the CRISPR-associated proteins (Cas) construct an RNA-guided adaptive immune system (CRISPR-Cas) that has evolved in archaea and bacteria.[1,2] Among them, CRISPR-Cas12a system exhibits great promise in biosensing, since it not only specifically binds target DNA to perform site-specific (cis) cleavage but also displays the target bound-induced nonspecific collateral (trans) cleavage activity.[3,4] The collateral cleavage targets single-stranded DNA (ssDNA) labeled with a fluorophore and quencher at each end (referred to as an F−Q reporter), enormously improving the detection sensitivity.[5−8] Taking advantage of this property, a variety of CRISPR-Cas12a-based biosensors, such as HOLMES (One hour low-cost multipurpose highly efficient system)[9] and DETECTR (DNA endonuclease-targeted CRISPR trans reporter),[10] have been developed for highly sensitive detection of nucleic acids. Despite these achievements, the application of CRISPR-Cas12a-based biosensors for the non-nucleic acid target detection is still in its infancy. To fully explore the potential of CRISPR technologies in biosensing applications, the target DNA (hereafter called DNA activator) recognition event need be converted into the trans-cleavage activity regulation of Cas12a.[11−13] By coupling functional nucleic acids (FNAs, e.g., DNAzyme and aptamer), researchers have developed CRISPR-Cas12a-based biosensors for the detection of ions, small molecules, and proteins.[11,14,15] However, these biosensors often require tedious and complicated engineering of either crRNA or a DNA activator that regulates the Cas12a function. Therefore, there is a strong need for designing novel strategies to manipulate the trans-cleavage activity of Cas12a effector without any complex design.

Previous studies have demonstrated that some proteins can nonspecifically bind DNA using electrostatic and hydrophobic interactions and form a strong spatial block, resulting in a "locked state".[16,17] This discovery underlines the widespread nature of protein-induced nonspecific DNA binding and offers an approach for regulating protein activity.[18,19] Given the fact that Cas12a is a protein complex, there is a possibility that ssDNA can nonspecifically bind Cas12a to inhibit the following DNA activator binding. Here, we made an observation that the state of Cas12a ("locked" or "activated") is dependent on the length of the nonspecifically adsorbed ssDNA, thus providing a novel avenue for controllably

Received: December 29, 2024
Revised: March 31, 2025
Accepted: April 15, 2025

ACS Publications © XXXX American Chemical Society

Scheme 1. Schematic Illustration of the tRCD/RCS-Cas12a Biosensor for Non-Nucleic Acid Target Detection



regulating the Cas12a function. This strategy avoids the complex engineering of crRNA and DNA activator, therefore simplifying the design of CRISPR-Cas12a biosensors for non-nucleic acid target detection.

As we will show for the first time in this work, integrating the CRISPR-Cas12a system with a ssDNA assembly made of a trans-acting RNA-cleaving DNAzyme (tRCD) and its RNA/DNA chimeric substrate (RCS) has led to the design of a novel biosensing strategy. We termed this approach tRCD/RCS-Cas12a. The biosensor features two components: CRISPR-Cas12a for the fluorescence signal generation; tRCD/RCS assembly for the non-nucleic acid target recognition[20] and CRISPR-Cas12a activity regulation. In the absence of the target, the tRCD/RCS assembly prevents CRISPR-Cas12a from performing its function to produce the fluorescence signal. The presence of the target, however, triggers the release of tRCD from Cas12a, cleaving the RCS into two short sequences.[21] This in turn makes Cas12a available for DNA activator binding, thus restoring the CRISPR-Cas12a function. Combining these innovative features enables us to successfully analyze patient samples with urinary tract infections (UTIs) caused by *Escherichia coli* (*E. coli*, EC). Furthermore, this approach can be adopted for the detection of *Burkholderia gladioli* (*B. gladioli*, BG) by using the suitable tRCD/RCS assembly. We envision that the described biosensing strategy will find useful applications in the detection of wide-ranging non-nucleic acid targets.[22]

EXPERIMENTAL SECTION

Chemicals and Reagents. All DNA oligonucleotides were purchased from Sangon Biotech (Shanghai, China) and purified by 10% denaturing (8 M urea) polyacrylamide gel electrophoresis (dPAGE) or high-performance liquid chromatography (HPLC). The RNA oligonucleotides were purchased from Generay Biotech (Shanghai, China) and purified by HPLC. The sequences of all DNA and RNA oligonucleotides are provided in Table S1, Supporting Information. Engen Lba Cas12a protein was purchased from New England Biolabs. Enzyme-free water was purchased from TaKaRa Biomedical Technology (Dalian, China). Sodium chloride (NaCl), potassium chloride (KCl), magnesium chloride ($MgCl_2$), and other chemicals were purchased from Sangon Biotech Co., Ltd. (Shanghai, China).

1× NEBuffer: 20 mM Tris−HCl, 100 mM KCl, 5 mM $MgCl_2$, 1 mM DTT, 5% glycerol, and 50 μg/mL Heparin, pH 7.5.

1× Selection buffer (1× SB): 50 mM HEPES, 150 mM NaCl, 15 mM $MgCl_2$, and 0.01% Tween 20, pH 7.5.

1× Reaction buffer (1× RB): 50 mM Pramipexole Impurity, 15 mM $MgCl_2$, and 0.01% Tween 20, pH 7.5.

Effect of ssDNA on CRISPR-Cas12a Function. Cis-cleavage activity. Two μL of 10× NEBuffer, 0.3 μL of 10 μM crRNA-7-2, 0.3 μL of 10 μM Cas12a protein, and 12−70 nt of ssDNA sequences (S1−S7) at varying final concentrations (0, 0.05, 0.1, 0.5, 1, and 5 μM) were mixed and diluted to 20 μL using sterile enzyme-free water. After incubation at 37 °C for 10 min, 0.15 μL of 10 μM 5′ FAM TS-7-2 (DNA activator) was added into the above mixture and mixed with a pipet. Following incubation at 37 °C for 60 min, the obtained product was analyzed by 10% dPAGE and quantified using ImageJ software.

Trans-Cleavage Activity. Ten μL portion of 10× NEBuffer, 0.3 μL of 10 μM crRNA-7-2, 0.3 μL of 10 μM Cas12a protein, and S1−S7 with different final concentrations (0, 1, 2.5, and 5 μM) were mixed and diluted to 100 μL using sterile enzyme-free water. After incubation at 37 °C for 10 min, 0.75 μL of 10 μM TS-7-2 and 2 μL of 10 μM F−Q reporter were added and transferred into a 96-well plate for real-time fluorescence measurement. The fluorescence at $\lambda_{ex}/\lambda_{em}$ = 485 nm/520 nm was recorded every minute for 120 min using a Cary Eclipse fluorescence spectrophotometer (Agilent, US).

Cleavage of RCS by tRCD. 50 μM *E. coli*-responding tRCD (tRCD-EC) (or *B. gladioli*-responding tRCD, named tRCD-BG) was incubated with 2.5 μM RCS-EC (or RCS-BG) in 50 μL of 1× SB, and the mixture was heated at 90 °C for 2 min. After cooling at room temperature (RT) for 10 min, 10 μL of crude intracellular mixture of *E. coli* (CIM-EC) or crude extracellular mixture of *B. gladioli* (CEM-BG) was added and incubated at RT for 60 min. The obtained cleavage product was analyzed by 10% dPAGE and quantified using ImageJ software.

Sensitivity and Specificity of tRCD/RCS-Cas12a. 2.5 μM RCS-EC or RCS-BG, 2.5 μM tRCD-EC or tRCD-BG, and 12.5 μL of 4× SB were mixed and diluted to 50 μL using sterile enzyme-free water and heated at 90 °C for 2 min. After being cooled at RT for 10 min, 50 μL of CIM-EC (or CEM-BG) with different concentrations (10^7, 10^6, 10^5, 10^4, 10^3, 10^2, 10, and 0 CFU/mL), 10 μL of 10× NEBuffer, 1.5 μL of 10 μM

https://doi.org/10.1021/acs.analchem.4c07081
Anal. Chem. XXXX, XXX, XXX−XXX

crRNA, and 1.5 μL of 10 μM Cas12a were added (final volume: 100 μL) and then incubated at 37 °C for 10 min. Finally, 0.75 μL of 10 μM TS-7-2 and 2 μL of 10 μM F−Q reporter were added. Fluorescence intensity at $\lambda_{ex}/\lambda_{em}$ = 485 nm/520 nm was recorded every minute for 120 min. For studying the specificity, CIMs from different bacteria (10^7 CFU/mL) were used.

RESULTS AND DISCUSSION

Working Principle of tRCD/RCS-Cas12a. The working principle of our design is illustrated in Scheme 1. The biosensing sensing system features CRISPR-Cas12a as a signal transducer and an ssDNA assembly made of a tRCD and its long RCS as the target recognition element. Upon mixing, the ssDNA assembly is expected to nonspecifically adsorb onto the Cas12a using electrostatic and hydrophobic interactions. The formation of a tight tRCD/RCS-Cas12a structure serves to mask the DNA activator binding domain, making it unavailable for activating the CRISPR-Cas12a. Note that the observed inhibition was highly dependent on the given length of the ssDNA assembly. A complete arrest of CRISPR-Cas12a can be obtained using a longer ssDNA assembly. When the target is introduced, tRCD prefers to bind to the target, allowing for the cleavage of RCS into short fragments. This resulted in the release of CRISPR-Cas12a for recognizing the DNA activator, thus triggering Cas12a-mediated trans-cleavage of the F−Q reporter. The detection of the target is, therefore, easily converted to the generation of a strong fluorescence signal.

Effects of ssDNA on CRISPR-Cas12a Function. The conceptual cornerstone of this work is the assumption that nonspecific ssDNA binding efficiently blocks the CRISPR-Cas12a function. It was demonstrated that nonspecific binding of ssDNA to Cas12a is mainly through: (1) the negatively charged phosphate backbone of ssDNA interacts with the central large positively charged channel formed by the Cas12a−crRNA complex and (2) ssDNA engages with the oligonucleotide-binding domain that harbors a looped-out helical domain (LHD) of the CRISPR system. We first studied the effect of ssDNA on the cis-cleavage activity of the CRISPR-Cas12a system. A fluorophore-labeled DNA activator (named 5′ FAM TS-7-2) was used. ssDNA sequences with different lengths (S1−S7) (Figure S1 and Supporting Information) were carefully designed to avoid hybridization with crRNA or the DNA activator. When ssDNA was used at 1 μM, the cis-cleavage yield (%) was decreased from 92% to 50% (Figures 1A and S1, Supporting Information) with extending the length of ssDNA from 12 nt (S1) to 70 nt (S7). Furthermore, the observed inhibition effect was highly dependent on the concentration of ssDNA. Increasing the concentration of S7 to 0.5, 1, and 5 μM resulted in decreased cleavage yield to 72%, 50%, and 1%, respectively. We next tested whether ssDNA could inhibit trans-cleavage by Cas12a using an F−Q reporter (Figures 1B and S2, Supporting Information). No significant fluorescence increase was observed for CRISPR-Cas12a in the presence of 5 μM S4 (40 nt), 5 μM S5 (50 nt), 2.5 μM S6 (60 nt), and 1 μM S7 (70 nt). In contrast, S1 (10 nt), S2 (20 nt), and S3 (30 nt) cannot inactivate the trans F−Q reporter cleavage activity of Cas12a even at higher concentrations (5 μM), resulting in a dramatic time-dependent increase in fluorescence.

We further examined whether the sequence context played important roles in delivering an inhibitory effect on CRISPR-Cas12a. Three ssDNA sequences including poly(adenine) (pA70), poly(thymine) (pT70), and a DNA pool (made of a random sequence of 70 nucleotides) were tested. The calculated cis-cleavage yield (%) for pA70, pT70, and DNA pool (final concentration of 1 μM) was 94%, 0%, and 41%, respectively (Figure S3, Supporting Information), suggesting that the sequence context can influence the outcome of CRISPR-Cas12a arresting. For the DNA pool, the cis-cleavage yield (%) decreased to 0% with increasing concentration to 5 μM. In sharp contrast, pA70 cannot efficiently inhibit the trans-cleavage by Cas12a using the F−Q reporter. For comparison, we found that pT70 and the DNA pool robustly inhibited the trans-acting DNase activity of Cas12a even at a lower concentration (1 μM).

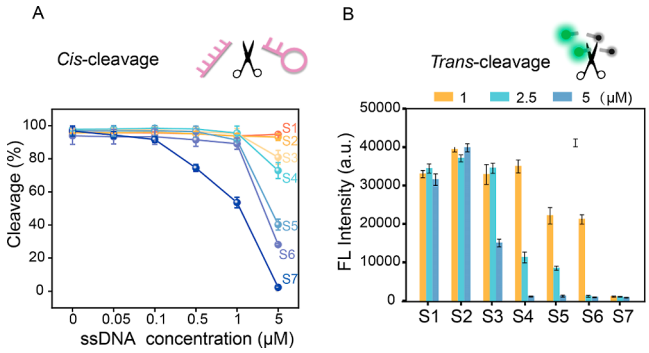


Figure 1. Effects of ssDNA (S1−S7) on (A) cis- and (B) trans-cleavage activities of CRISPR-Cas12a. The error bars represent standard deviations of three independent experiments. The data are expressed as mean ± s.d.

Feasibility of tRCD/RCS-Cas12a. We next examined the possibility of exploiting tRCD/RCS-Cas12a for biosensing applications. In theory, the tRCD/RCS-Cas12a reaction should be compatible with any of the RCDs. We first used tRCD-EC (26 nt), which was found to be activated by protein molecules secreted specifically by *E. coli* and isolated from random-sequence DNA libraries via in vitro selection.[23] RCS-EC (40 nt) was designed to contain a poly(thymine) (T12) sequence at the 5′ end. The trans-acting tRCD-EC interacts with RCS-EC through one Watson−Crick binding arm (Figure 2A). Upon target binding, tRCD-EC can be activated to catalyze the cleavage of a lone RNA linkage (R) embedded in RCS-EC: attack of an RNA 2′-hydroxyl group on the adjacent phosphodiester linkage resulted in the production of two short cleaved fragments (Figure S4, Supporting Information).

We evaluated the effect of the RCS-EC concentration on the function of the CRISPR systems. As shown in Figure 2B, cis-cleavage of the DNA activator by CRISPR-Cas12a was not observed with the increase of RCS-EC concentration from 0.25 to 1 μM. Furthermore, the addition of RCS-EC (2.5 μM) completely arrested the trans-cleavage reaction using FQ-ssDNA, as no fluorescence increase was observed (Figure 2C). The ratio of tRCD-EC/RCS-EC was set at 1:1 to ensure the cleavage of RCS-EC by tRCD-EC in the presence of *E. coli*, resulting in higher cleavage activity with 56% final cleavage yield (Figure S5, Supporting Information). As expected, tRCD-EC-induced cleavage of RCS-EC led to the restoration of CRISPR-Cas12a for trans-ssDNA cleavage of the F−Q reporter (Figure 2D). Taken together, these results verify the feasibility of designing a tRCD/RCS-Cas12a biosensor by taking advantage of target-induced switching between a tRCD/RCS/CRISPR-Cas12a assembly and a DNA activator/CRISPR-Cas12a complex.

https://doi.org/10.1021/acs.analchem.4c07081
Anal. Chem. XXXX, XXX, XXX−XXX

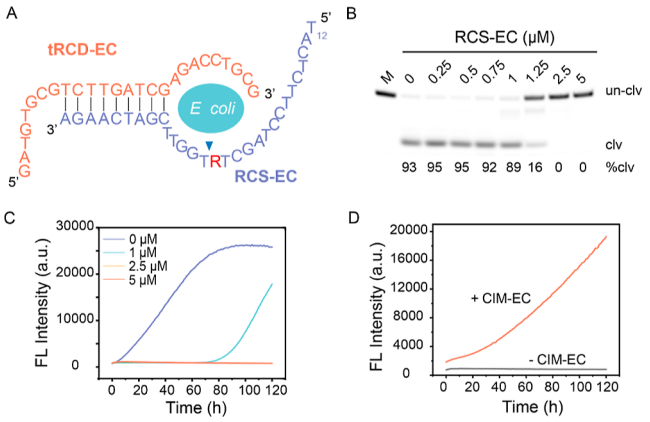


Figure 2. (A) Schematic structure of tRCD-EC and RCS-EC. R: adenine ribonucleotide. Filled triangle: cleavage site. (B) 10% dPAGE analysis of the cis-cleavage activity of CRISPR-Cas12a with varying RCS-EC concentrations. Reaction time: 1 h, M: marker, clv: cleaved, unclv: uncleaved, %clv: cleavage percentage. (C) Fluorescence responses of CRISPR-Cas12a-catalyzed trans-cleavage of the F−Q reporter in the presence of different concentrations of RCS-EC. (D) Fluorescence responses of CRISPR-Cas12a-catalyzed trans-cleavage of the F−Q reporter with a ratio of tRCD-EC to RCS-EC at 1:1 in the absence and presence of CIM-EC (10^6 CFU/mL).

Performance of tRCD/RCS-Cas12a. To demonstrate the analytical utility of the proposed approach, the tRCD/RCS-Cas12a reactions were monitored in real time with an F−Q reporter that was cleaved by Cas12a to generate fluorescence. It was able to produce fluorescent signals proportional to the concentration of *E. coli* (Figure 3A). The limit of detection

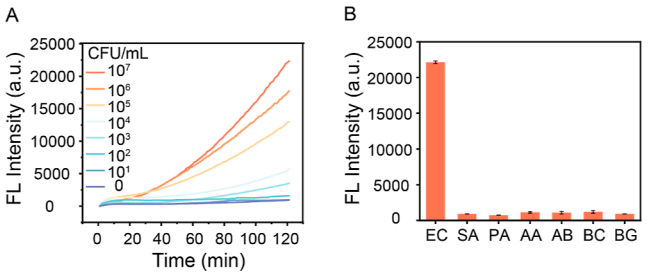


Figure 3. (A) Fluorescence response of the tRCD/RCS-Cas12a biosensor against different concentrations of *E. coli*. (B) Specificity of the tRCD/RCS-Cas12a biosensor. The error bars represent standard deviations of three independent experiments. The data are expressed as mean ± s.d.

(LOD, defined as 3σ, σ = standard deviation of the blank samples) was determined to be 10^2 CFU/mL. Therefore, our tRCD/RCS-Cas12a biosensor offers a detection sensitivity that is 100 times better than that of the DNAzyme method without signal amplification.[23] Furthermore, no increase of fluorescence was observed when the system was tested with unintended targets (Figure 3B): *Staphylococcus aureus* (*S. aureus*, SA), *Pseudomonas aeruginosa* (*P. aeruginosa*, PA), *Acinetobacter actinomycetemcomitans* (*A. actinomycetemcomitans*, AA), *Acinetobacter baumannii* (*A. baumannii*, AB), *Bacillus cereus* (*B. cereus*, BC), and *B. gladioli* (*B. gladioli*, BG). Compared with current CRISPR-based methods for bacterial detection, our tRCD/RCS-Cas12a biosensor offers better sensitivity, shorter assay time, and ease of use (Table S2).

Clinical Sample Analysis. We investigated the applicability of the tRCD/RCS-Cas12a biosensor in the clinical diagnosis of UTIs caused by *E. coli*. The overall assay procedure, shown in Figure 4A, includes: (i) Bacterial

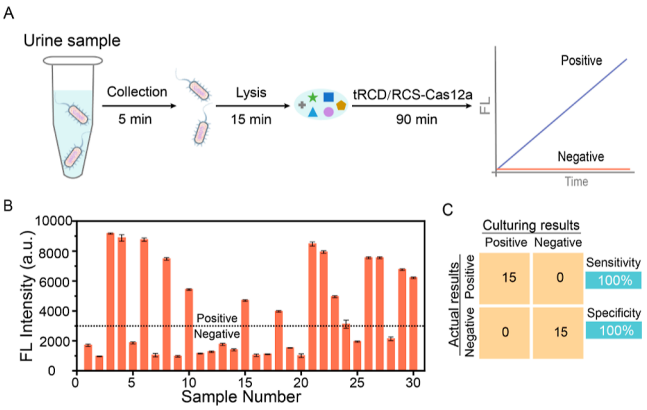


Figure 4. tRCD/RCS-Cas12a biosensor for *E. coli* detection in clinical samples. (A) Schematic illustration of *E. coli* detection workflow from the sample to result. (B) Fluorescence responses of *E. coli* detection in 30 clinical urine samples using tRCD/RCS-Cas12a. The error bars represent standard deviations of three independent experiments. The data are expressed as mean ± s.d. (C) Performance characteristics of the tRCD/RCS-Cas12a biosensor for *E. coli* detection in clinical samples.

collection, cells in clinical samples were collected by centrifugation for 5 min, (ii) Bacterial lysis, the CIM-EC was extracted by ultrasound within 15 min, and (iii) tRCD/RCS-Cas12a reaction (90 min). The fluorescence signal was recorded. Using this procedure, we analyzed 15 *E. coli* culturing-positive and 15 *E. coli* culturing-negative urine samples (Figure S6, Supporting Information). As shown in Figure 4B, we found that the fluorescence intensities of 15 samples (No. 3, 4, 6, 8, 10, 15, 18, 21, 22, 23, 24, 26, 27, 29 and 30), were higher. Using the clinical threshold of 1×10^3 CFU/mL, we achieved a clinical sensitivity of 100% and a clinical specificity of 100% without the need for bacterial culture (Figure 4C). Furthermore, the total sample-to-result time was 2 h for our sensor, compared with 15 h needed for the currently urine cultures. Therefore, our proposed tRCD/RCS-Cas12a biosensor can be potentially used for infectious disease diagnostics.

tRCD/RCS-Cas12a for *B. gladioli* Detection. To confirm the general applicability of the approach, we designed tRCD/RCS-Cas12a for the detection of *B. gladioli*. The original tRCD/RCS-Cas12 was altered simply through the replacement of the tRCD-EC with a new tRCD, named tRCD-BG, a previously reported tRCD that can only be activated by *B. gladioli*.[24] Its corresponding RCS-BG contains 38 nucleotides, distributed as an RNA/DNA chimeric substrate at the 3′ end and a poly(thymine) (T12) sequence at the 5′ end. As illustrated in Figure 5A, two DNA molecules, tRCD-BG and RCS-BG, were used to set up the tRCD/RCS-Cas12a system. It was observed that tRCD-BG was indeed able to cleave RCS-BG in the presence of CEM-BG, as confirmed by the appearance of the cleavage fragments (Figure 5B). The tRCD/RCS-Cas12a reaction mixture was then subjected to quantitative analysis by fluorescence measurement in the presence of different concentrations of CEM-BG (Figure 5C). The LOD was estimated to be 10^2 CFU/mL. This represents a

https://doi.org/10.1021/acs.analchem.4c07081
Anal. Chem. XXXX, XXX, XXX−XXX

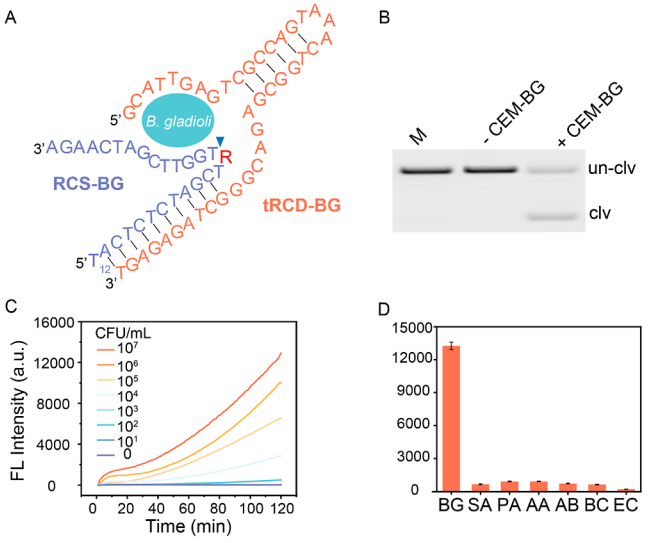


Figure 5. (A) Schematic structure of tRCD-BG and RCS-BG. R: adenine ribonucleotide. Filled triangle: cleavage site. (B) 10% dPAGE analysis of the cleavage reaction mixtures of the tRCD-BG/RCS-BG in the presence CEM-BG. M: marker, clv: cleaved, unclv: uncleaved, Reaction time: 1 h. (C) Fluorescence responses of the tRCD/RCS-Cas12a biosensor against different concentrations of *B. gladioli*. (D) Specificity of tRCD/RCS-Cas12a. Reaction time: 2 h. The error bars represent standard deviations of three independent experiments. The data are expressed as mean ± s.d.

10-fold improvement in LOD over the traditional tRCD assay.[24] Besides the high sensitivity, the tRCD/RCS-Cas12a biosensor also exhibited excellent selectivity for its cognate target. No fluorescence increase was observed when each system was tested with unintended targets: SA, AB, PA, AA, BC, and EC (Figure 5D).

CONCLUSIONS

In conclusion, we have made a novel observation that the nonspecific binding of ssDNA assembly to Cas12a can efficiently arrest CRISPR-Cas12a functions. We have further demonstrated that such CRISPR-Cas12a arrest can be uniquely exploited for the design of a biosensing system using tRCD. The system begins with a tRCD/RCS assembly that inhibits the CRISPR-Cas12a functions, whereas target-mediated cleavage of RCS by tRCD frees up the Cas12a for activating the following CRISPR-Cas12a reactions. To our knowledge, this work serves as the first example of nonspecific ssDNA-controlled CRISPR-Cas functions without tedious crRNA engineering. The broad utility of the tRCD/RCS-Cas12a system is illustrated though engineering two sensors that are capable of achieving sensitive detection of *E. coli* and *B. gladioli*. Clinical evaluation of this biosensor demonstrated a clinical sensitivity of 100% and a specificity of 100% in analyzing 30 patient urine samples. Given that there is a wide variety of RCDs,[25] as well as RNA-cleaving ribozymes currently available that can be activated by metal ions, small molecules or bacterial pathogens, and new RCDs that can be directly evolved by in vitro selection, we envision the described system will find diverse applications for the detection of different molecules of interest in chemical biology, clinical diagnostics, and environmental monitoring. Future work will develop low-cost and fully integrated paper device by integrating paper-based sample treatment and cell lysis, paper-based biosensor, and portable readout for point-of-care detection of pathogenic bacteria in resource-limited settings.[26,27]

ASSOCIATED CONTENT

Supporting Information

The Supporting Information is available free of charge at https://pubs.acs.org/doi/10.1021/acs.analchem.4c07081.

Additional experimental details including preparation of CIM and CEM; tRCD/RCS-Cas12a; and culturing method for clinical sample analysis (PDF)

AUTHOR INFORMATION

Corresponding Authors

Yangyang Chang − *School of Environmental Science and Technology, Dalian POCT Laboratory, Key Laboratory of Industrial Ecology and Environmental Engineering (Ministry of Education), Dalian University of Technology, Dalian 116024, China;* orcid.org/0000-0001-7103-2171; Email: yychang@dlut.edu.cn

Meng Liu − *School of Environmental Science and Technology, Dalian POCT Laboratory, Key Laboratory of Industrial Ecology and Environmental Engineering (Ministry of Education), Dalian University of Technology, Dalian 116024, China;* orcid.org/0000-0003-3114-9003; Email: mliu@dlut.edu.cn

Authors

Yue Liu − *School of Environmental Science and Technology, Dalian POCT Laboratory, Key Laboratory of Industrial Ecology and Environmental Engineering (Ministry of Education), Dalian University of Technology, Dalian 116024, China*

Yunping Wu − *School of Environmental Science and Technology, Dalian POCT Laboratory, Key Laboratory of Industrial Ecology and Environmental Engineering (Ministry of Education), Dalian University of Technology, Dalian 116024, China*

Yi Liu − *The Affiliated Central Hospital, Dalian University of Technology, Dalian 116000, China*

Qiang Zhang − *School of Bioengineering, Key Laboratory of Bio-Intelligent Manufacturing (Ministry of Education), Dalian University of Technology, Dalian 116024, China*

Hong Yuan − *The Affiliated Central Hospital, Dalian University of Technology, Dalian 116000, China*

Shen Li − *The Affiliated Central Hospital, Dalian University of Technology, Dalian 116000, China*

Zhi Li − *Clinical Laboratory, Dalian Municipal Central Hospital, Dalian 116000, China*

Bo Wang − *Clinical Laboratory, Dalian Municipal Central Hospital, Dalian 116000, China*

Complete contact information is available at: https://pubs.acs.org/10.1021/acs.analchem.4c07081

Author Contributions

⊥Yue Liu, Yunping Wu, and Yi Liu contributed equally to this work. All authors have given approval to the final version of the manuscript.

Notes

The authors declare no competing financial interest.

https://doi.org/10.1021/acs.analchem.4c07081
Anal. Chem. XXXX, XXX, XXX−XXX

■ ACKNOWLEDGMENTS

We are grateful for financial support from the National Natural Science Foundation of China (NSFC; 22176024), the National Key R&D Program of China (2023YFC3205804), and the Dalian Science and Technology Innovation Fund (2023YGZD02 and 2023YGZD08).

■ REFERENCES

(1) Horvath, P.; Barrangou, R. *Science* **2010**, *327* (5962), 167−170.
(2) Cong, L.; Ran, F. A.; Cox, D.; Lin, S.; Barretto, R.; Habib, N.; Hsu, P. D.; Wu, X.; Jiang, W.; Marraffini, L. A.; Zhang, F. *Science* **2013**, *339* (6121), 819−823.
(3) Weng, Z.; You, Z.; Yang, J.; Mohammad, N.; Lin, M.; Wei, Q.; Gao, X.; Zhang, Y. *Angew. Chem., Int. Ed.* **2023**, *62* (17), No. e202214987.
(4) Wang, B.; Wang, R.; Wang, D.; Wu, J.; Li, J.; Wang, J.; Liu, H.; Wang, Y. *Anal. Chem.* **2019**, *91* (19), 12156−12161.
(5) Stella, S.; Mesa, P.; Thomsen, J.; Paul, B.; Alcón, P.; Jensen, S. B.; Saligram, B.; Moses, M. E.; Hatzakis, N. S.; Montoya, G. *Cell* **2018**, *175* (7), 1856−1871.
(6) Wang, J. Y.; Doudna, J. A. *Science* **2023**, *379* (6629), No. eadd8643.
(7) Wang, Y.; Ke, Y.; Liu, W.; Sun, Y.; Ding, X. *ACS Sens.* **2020**, *5* (5), 1427−1435.
(8) Zhao, Z.; Xiong, Q.; Zhu, Y.; Zhang, C.; Li, Z.; Chen, Z.; Zhang, Y.; Deng, X.; Tao, Y.; Xu, S. *Anal. Chem.* **2025**, *97* (1), 1019−1027.
(9) Li, S.-Y.; Cheng, Q.-X.; Wang, J.-M.; Li, X.-Y.; Zhang, Z.-L.; Gao, S.; Cao, R.-B.; Zhao, G.-P.; Wang, J. *Cell Discovery* **2018**, *4* (1), 20.
(10) Chen, Y.; Xu, X.; Wang, J.; Zhang, Y.; Zeng, W.; Liu, Y.; Zhang, X. *Anal. Chem.* **2022**, *94* (27), 9724−9731.
(11) Liang, M.; Li, Z.; Wang, W.; Liu, J.; Liu, L.; Zhu, G.; Karthik, L.; Wang, M.; Wang, K.-F.; Wang, Z.; Yu, J.; Shuai, Y.; Yu, J.; Zhang, L.; Yang, Z.; Li, C.; Zhang, Q.; Shi, T.; Zhou, L.; Xie, F.; Dai, H.; Liu, X.; Zhang, J.; Liu, G.; Zhuo, Y.; Zhang, B.; Liu, C.; Li, S.; Xia, X.; Tong, Y.; Liu, Y.; Alterovitz, G.; Tan, G.-Y.; Zhang, L.-X. *Nat. Commun.* **2019**, *10* (1), 3672.
(12) English, M. A.; Soenksen, L. R.; Gayet, R. V.; de Puig, H.; Angenent-Mari, N. M.; Mao, A. S.; Nguyen, P. Q.; Collins, J. J. *Science* **2019**, *365* (6455), 780−785.
(13) Xiong, Y.; Zhang, J.; Yang, Z.; Mou, Q.; Ma, Y.; Xiong, Y.; Lu, Y. *J. Am. Chem. Soc.* **2020**, *142* (1), 207−213.
(14) van Beljouw, S. P. B.; Sanders, J.; Rodríguez-Molina, A.; Brouns, S. J. J. *Nat. Rev. Microbiol.* **2023**, *21* (1), 21−34.
(15) Cheng, X.; Li, Y.; Kou, J.; Liao, D.; Zhang, W.; Yin, L.; Man, S.; Ma, L. *Biosens. Bioelectron.* **2022**, *215*, 114559.
(16) Liu, X.; Zhang, L.; Xiu, Y.; Gao, T.; Huang, L.; Xie, Y.; Yang, L.; Wang, W.; Wang, P.; Zhang, Y.; Yang, M.; Feng, Y. *Nucleic Acids Res.* **2021**, *49* (17), 10178−10191.
(17) Xie, Y.; Zhang, L.; Gao, Z.; Yin, P.; Wang, H.; Li, H.; Chen, Z.; Zhang, Y.; Yang, M.; Feng, Y. *Nat. Chem. Biol.* **2022**, *18* (6), 670−677.
(18) Kundert, K.; Fraser, J. S. *Nature* **2020**, *587* (7833), 199−200.
(19) Fosado, Y. A.; Howard, J.; Weir, S.; Noy, A.; Leake, M. C.; Michieletto, D. *Phys. Rev. Lett.* **2023**, *130* (5), 058203.
(20) Liu, M.; Chang, D.; Li, Y. *Acc. Chem. Res.* **2017**, *50* (9), 2273−2283.
(21) Chang, D.; Zakaria, S.; Esmaeili Samani, S.; Chang, Y.; Filipe, C. D.; Soleymani, L.; Brennan, J. D.; Liu, M.; Li, Y. *Acc. Chem. Res.* **2021**, *54* (18), 3540−3549.
(22) Dong, De.; Ren, K.; Qiu, X.; Zheng, J.; Guo, M.; Guan, X.; Liu, H.; Li, N.; Zhang, B.; Yang, D.; Ma, C.; Wang, S.; Wu, D.; Ma, Y.; Fan, S.; Wang, J.; Gao, N.; Huang, Z. *Nature* **2016**, *532*, 522−526.
(23) Ali, M. M.; Aguirre, S. D.; Lazim, H.; Li, Y. *Angew. Chem., Int. Ed.* **2011**, *50*, 3751−3754.
(24) Li, X.; Chang, Y.; Wu, Y.; Liu, M. *Chem. Sci.* **2024**, *15* (8), 2996−3002.
(25) McConnell, E. M.; Cozma, I.; Mou, Q.; Brennan, J. D.; Lu, Y.; Li, Y. *Chem. Soc. Rev.* **2021**, *50*, 8954−8994.
(26) Zhang, G.; Wu, Y.; Xue, W.; Wang, D.; Chang, Y.; Liu, M. *Chem. Commun.* **2024**, *60*, 6741−6744.
(27) Xue, W.; Wu, Y.; Li, X.; Zhang, Q.; Wu, Y.; Chang, Y.; Liu, M. *Biosens. Bioelectron.* **2024**, *264*, 116687.

https://doi.org/10.1021/acs.analchem.4c07081
Anal. Chem. XXXX, XXX, XXX−XXX